

This is the accepted manuscript of the contribution published as:

Rübsam, H., Kirsch, F., Reimann, V., Erban, A., Kopka, J., Hagemann, M., Hess, W.R.,
Klähn, S. (2018):

The iron-stress activated RNA 1 (IsaR1) coordinates osmotic acclimation and iron starvation
responses in the cyanobacterium *Synechocystis* sp. PCC 6803

Environ. Microbiol. **20** (8), 2757 – 2768

The publisher's version is available at:

<http://dx.doi.org/10.1111/1462-2920.14079>

Title: The iron-stress activated RNA 1 (IsaR1) coordinates osmotic acclimation and iron starvation responses in the cyanobacterium *Synechocystis* sp. PCC 6803

Henriette Rübsam¹, Friedrich Kirsch², Viktoria Reimann¹, Alexander Erban³, Joachim Kopka³, Martin Hagemann², Wolfgang R. Hess¹, Stephan Klähn^{1*}

¹University of Freiburg, Faculty of Biology, Genetics and Experimental Bioinformatics, Schänzlestr. 1, D-79104 Freiburg, Germany

²University of Rostock, Institute of Biological Sciences, Plant Physiology department, A.-Einstein-Str. 3, D-18059 Rostock, Germany

³Max-Planck-Institute of Molecular Plant Physiology, Department of Molecular Physiology: Applied Metabolome Analysis, Am Mühlenberg 1, D-14476 Potsdam-Golm, Germany

Corresponding author(*):

Stephan Klähn
Genetics & Experimental Bioinformatics
University of Freiburg
Institute of Biology III
Schänzlestrasse 1
D-79104 Freiburg, Germany

Phone: +49 (0) 761 203-2789

Email: stephan.klaehn@biologie.uni-freiburg.de

Running title: The role of IsaR1 in osmoregulation of cyanobacteria

This article has been accepted for publication and undergone full peer review but has not been through the copyediting, typesetting, pagination and proofreading process which may lead to differences between this version and the Version of Record. Please cite this article as an 'Accepted Article', doi: 10.1111/1462-2920.14079

Originality-Significance Statement

IsaR1 is a critically important riboregulator that affects the photosynthetic apparatus of cyanobacteria in response to iron starvation. However, here we demonstrate a previously hidden function of IsaR1 and uncover a dual role of this small RNA. In addition to the main iron-related set of target genes, IsaR1 also interferes with the osmoregulation of the important cyanobacterial model strain *Synechocystis* sp. PCC 6803. To counterbalance low water potential of saline or aride environments bacteria generally accumulate compatible solutes - one of the major factors to cope with abiotic stresses. Many salt-tolerant cyanobacteria including *Synechocystis* accumulate glucosylglycerol (GG) as main compatible solute. GG accumulation is essential at high salt concentrations but also demand high metabolic and energy resources. Apparently, IsaR1 is involved in regulating GG synthesis by targeting its key synthesizing enzyme. At a first glance the meaning of this regulation is not obvious since GG synthesis is not iron-dependent per se. However, high salinity and low iron availability often occur in combination, i.e. in marine environments. IsaR1 is involved in the integration of the responses to different environmental perturbations, slowing down the osmotic adaptation process in cells suffering from parallel iron starvation. With this work we present the first bacterial regulatory RNA involved in the regulation of compatible solute synthesis. The integrating function of IsaR1 provides a new paradigm for other sRNA regulators in bacteria.

Summary

In nature, microorganisms are exposed to multiple stress factors in parallel. Here, we investigated the response of the model cyanobacterium *Synechocystis* sp. PCC 6803 to simultaneous iron limitation and osmotic stresses. Iron is a major limiting factor for bacterial and phytoplankton growth in most environments. Thus, bacterial iron homeostasis is tightly regulated. In *Synechocystis*, it is mediated mainly by the transcriptional regulator FurA and the iron-stress activated RNA 1 (IsaR1). IsaR1 is an important riboregulator that affects the acclimation of the photosynthetic apparatus to iron starvation in multiple ways. Upon

Accepted Article

increases in salinity, *Synechocystis* responds by accumulating the compatible solute glucosylglycerol (GG). We show that IsaR1 overexpression causes a reduction in the *de novo* GG synthesis rate upon salt shock. We verified the direct interaction between IsaR1 and the 5'UTR of the *ggpS* mRNA, which in turn drastically reduced the *de novo* synthesis of the key enzyme for GG synthesis, glucosylglycerol phosphate synthase (GgpS). Thus, IsaR1 specifically interferes with the salt acclimation process in *Synechocystis*, in addition to its primary regulatory function. Moreover, the salt-stimulated GgpS production became reduced under parallel iron limitation in WT - an effect which is, however, attenuated in an *isaR1* deletion strain. Hence, IsaR1 is involved in the integration of the responses to different environmental perturbations and slows the osmotic adaptation process in cells suffering from parallel iron starvation.

Introduction

Microbial stress acclimation is well studied under controlled laboratory conditions, e.g., applying a single stress factor in a time-course experiment. However, in nature, multiple stress factors usually occur in parallel. For instance, iron is an essential nutrient because crucial biological processes rely on iron-containing proteins. Iron cofactors are required in electron transfer processes, e.g., in the photosynthetic apparatus, which is one of the most iron-rich cellular systems. Despite elemental iron being highly abundant on earth, virtually no free soluble iron is available (Wandersman and Delepelaire, 2004). Consequently, it is a major limiting factor for bacterial and phytoplankton growth in most aquatic environments. This problem is especially severe in marine environments (Boyd *et al.*, 2007; Moore *et al.*, 2013). An excess of the physiologically relevant Fe^{2+} is also detrimental, as it causes Fenton reactions that eventually lead to the formation of reactive oxygen species (Halliwell and Gutteridge, 1992). Therefore, microbial iron homeostasis is strictly regulated to ensure that its acquisition, storage and consumption are adjusted to meet demand and availability (Andrews *et al.*, 2003). In many bacteria, this regulation is primarily mediated by the ferric-uptake regulator (Fur) (Hantke, 2001). In addition, Fur-repressed small RNAs (sRNAs) have been identified in many bacteria and contribute to the regulation of iron homeostasis at the post-transcriptional level (Massé and Gottesman, 2002; Wilderman *et al.*, 2004; Georg *et al.*, 2017).

In addition to iron limitation, organisms living in a marine environment have to cope with high salinity, which is another major abiotic factor that affects biological processes. Thus, low iron availability and high salinity often occur in combination. Moreover, both iron availability and salinity can strongly fluctuate in parallel, e.g., during estuarine mixing, where large-scale and rapid removal of iron from river water occurs while salinity increases (Boyle *et al.*, 1977). High salinity causes two major problems: (i) reduced water availability due to low external osmotic potential and (ii) the passive influx of inorganic ions due to a high concentration gradient. Both affect, for example, the hydration shell of proteins, which leads to reduced enzyme activity and metabolism. To maintain a low intracellular ion content as well as water

uptake, the typical acclimation strategy of bacteria combines active extrusion of inorganic ions with the accumulation of small organic, non-toxic molecules, also known as compatible solutes (Brown, 1976; Kempf and Bremer, 1998; Wood *et al.*, 2001; Hagemann, 2011; Lebre *et al.*, 2017).

With only a few exceptions, cyanobacteria that exhibit low salt tolerance accumulate sucrose and/or trehalose, whereas marine cyanobacterial strains with moderate salt tolerance use the heteroside glucosylglycerol (GG). The unicellular model strain *Synechocystis* sp. PCC 6803 (hereafter referred to as *Synechocystis*) was originally isolated from a freshwater habitat (Stanier *et al.*, 1971). However, it is a true euryhaline strain and can grow at salt concentrations twice those found in seawater (Reed and Stewart, 1985). It primarily accumulates GG by *de novo* synthesis in a two-step enzymatic reaction. First, the key enzyme GG-phosphate synthase (GgpS) catalyzes the glycosylation of glycerol-3-phosphate (G3P) by using ADP-glucose. The intermediate GG phosphate (GGP) is then dephosphorylated by a second enzyme, GGP phosphatase (GgpP) (Hagemann and Erdmann, 1994). GgpS is regulated at both the transcriptional and biochemical levels (Marin *et al.*, 2002; Novak *et al.*, 2011). Cells grown in freshwater medium only express basal levels of GgpS and are almost free of GG. However, upon salt shock, the internal GG level rapidly increases due to the activation of preformed enzymes and the salt-dependent initiation of expression. Two proteins have been proposed to be involved in the transcriptional regulation: GgpR and LexA (Klähn *et al.*, 2010; Kizawa *et al.*, 2016).

In addition to transcription factors, sRNAs can mediate important steps in the acclimation of bacteria to abiotic stresses at the posttranscriptional level (Waters and Storz, 2009). The iron-stress activated RNA 1 (IsaR1) in cyanobacteria plays a crucial regulatory role in the acclimation to iron starvation, affecting the photosynthetic apparatus in at least three ways (Georg *et al.*, 2017). Here, we show that the *ggpS* gene is a direct target of IsaR1 in addition to the reported iron-related genes. Thus, IsaR1 is the first known bacterial sRNA with a specific regulatory role in the synthesis of compatible solutes, which is fundamental to

osmoregulation. IsaR1 coordinates the cell responses to iron starvation with osmotic acclimation by effectively mediating an offset of the latter to prioritize the former.

Results

Modulation of IsaR1 abundance has a strong effect on *ggpS* expression levels

Recently, IsaR1 has been functionally verified as a crucial post-transcriptional regulator for iron homeostasis in cyanobacteria (Georg *et al.*, 2017). The IsaR1 regulon consists of more than 15 direct targets, including several Fe²⁺-containing proteins as well as proteins of the iron-sulfur cluster biogenesis system. Interestingly, upon pulse-overexpression of IsaR1 in *Synechocystis*, a slightly decreased abundance of the *ggpS* mRNA was also observed, despite the general low *ggpS* expression resulting from the experiments being performed with cells grown under freshwater conditions (Georg *et al.*, 2017). This observation raised the possibility that IsaR1 might also interact with the *ggpS* mRNA, interfering with its translation and thereby impacting the salt acclimation process in *Synechocystis*. To investigate this possibility, we used a previously generated IsaR1 overexpression strain (IsaR1OE) (Georg *et al.*, 2017), to analyze *ggpS* expression at the mRNA and protein levels compared to the wild-type strain (WT) (**Figure 1**). To ensure adequate *ggpS* expression, all strains were cultivated in the presence of 4% (w/v) NaCl throughout the experiment. In addition to the native *isaR1* gene on the chromosome, the IsaR1OE strain carried a plasmid with a second copy of the *isaR1* gene that was fused to the plastocyanin promoter (*PpetE*). This promoter is rapidly up-regulated when copper is added to the medium (Ghassemian *et al.*, 1994) and has repeatedly been used for controllable gene expression purposes in *Synechocystis* (Tan *et al.*, 2011; Klähn *et al.*, 2015; Englund *et al.*, 2016). Accordingly, low IsaR1 expression levels were observed in Cu²⁺-depleted medium in all strains, with a slightly increased IsaR1 abundance observed for the IsaR1OE strain compared to the WT strain (**Figure 1A**). This observation was probably caused by trace amounts of Cu²⁺ that were introduced with the high amounts of NaCl used in this experiment. Nevertheless, the *ggpS* expression level was similar in both strains. In contrast, 24 h after the addition of 2 µM Cu²⁺, drastically increased

IsaR1 levels were observed in IsaR1OE. Simultaneously, the *ggpS* mRNA abundance decreased by ~50% in the IsaR1OE strain compared to the WT strain (**Figure 1A**). It is frequently observed that sRNA:mRNA interactions alter the stability of the mRNA, which is due to direct or indirect effects (Caron *et al.*, 2010; Storz *et al.*, 2011). This has also been found in the PsrR1:*psaL* mRNA interaction in the here studied organism, where upon sRNA binding RNase E is recruited destabilizing the mRNA (Georg *et al.*, 2014). To verify that the changes observed for IsaR1OE also affected GgpS protein level, we performed immunoblots using a GgpS-specific antibody. Indeed, 24 h after the addition of Cu²⁺, the GgpS protein abundance was slightly reduced in the IsaR1OE strain compared to the WT strain (**Figure 1B**). We concluded that IsaR1 interferes with *ggpS* expression in *Synechocystis*.

IsaR1 directly interacts with the *ggpS* mRNA and impacts the translation of GgpS.

The regulon of IsaR1 contains several photosynthesis genes. Accordingly, IsaR1 overexpression is accompanied by a decrease in PSI yield and impacts cell physiology in multiple additional ways (Georg *et al.*, 2017). Therefore, we addressed the possibility that the altered *ggpS* abundance observed after inducing IsaR1 overexpression was caused indirectly. To this end, we performed experiments to verify a direct IsaR1:*ggpS* interaction. First, an interaction between IsaR1 and the *ggpS* 5'UTR was predicted near the *ggpS* start codon using the IntaRNA webserver (Busch *et al.*, 2008; Wright *et al.*, 2014) (**Figure 2A**). This location, which overlaps with the sequence elements needed for translation, is typical of regulation by non-coding RNAs (Storz *et al.*, 2011), which makes a direct effect very likely. Second, we aimed to verify the interaction of IsaR1 with the *ggpS* 5'UTR *in vitro*. To this end, we performed primer extension analysis showing that cDNA synthesis from a *ggpS* RNA is blocked in presence of IsaR1 at positions close to the predicted interaction sites (**Supplementary Figure S1**). And third, we used a well-established heterologous reporter system (Urban and Vogel, 2007; Corcoran *et al.*, 2012) to verify the direct interaction between IsaR1 and *ggpS* and assess its regulatory effect on GgpS translation *in vivo*. To this end, the *ggpS* 5'UTR was transcriptionally fused to the superfolder green fluorescent protein (*sgfp*) gene and was coexpressed with IsaR1 in *E. coli*. GFP fluorescence was measured *in*

vivo using a flow cytometer and strains with various combinations of plasmids (**Figure 2C**). Compared to a negative control, significant GFP fluorescence was observed in the strain carrying the *ggsS*-5'UTR::*sgfp* fusion, confirming that it was suitable to initiate translation in *E. coli* (**Figure 2C**). However, co-expression of IsaR1 decreased the GFP fluorescence almost 3-fold, thus confirming a diminished translation of *sgfp* due to an interaction of IsaR1 with the *ggsS* 5'UTR. Finally, to verify that IsaR1 indeed binds to the predicted site upstream of the start codon (**Figure 2A**), point mutations were established in the seed region that is essential for the *ggsS*-IsaR1 interaction (**Figure 2B**). We chose point mutations that did not change the secondary structure of the respective RNAs. Moreover, the point mutation in the *ggsS* mRNA (a C to G exchange at position +354 with respect to the transcriptional start site +1) did not affect the translation initiation, since a similar fluorescence was observed compared to the strain carrying the native *ggsS*-5'UTR::*sgfp* fusion (**Figure 2C**). However, mutation of either IsaR1 (at position +19, an exchange of G to C) or *ggsS* led to an increased translation rate, as a diminished *sgfp* repression (2-fold) was observed compared to the full repression (3-fold) (**Figure 2D**). In contrast, the combination of the complementary mutations restored the full repression. These results confirmed a direct interaction between IsaR1 and the *ggsS* mRNA. Thus, the decreased *ggsS* transcript and GgpS protein levels in *Synechocystis* (**Figure 1**) are a direct consequence of IsaR1 binding to the *ggsS* mRNA, affecting its stability and translation.

IsaR1 overexpression causes a delay in GgpS protein expression upon salt shock.

Pulse-overexpression of IsaR1 in *Synechocystis* led to a strong decrease of *ggsS* mRNA levels, whereas the effect was rather low at the protein level. In our initial experiment, the *ggsS* gene was already highly expressed due to long-term cultivation in presence of 4% NaCl. It is thus possible that the effects of IsaR1 pulse-overexpression on *ggsS* translation were masked because of high GgpS stability. Therefore, we investigated GgpS accumulation during the transition to high salinity, i.e., immediately after the addition of salt. To this end, WT and IsaR1OE cells were first pre-cultivated in Cu²⁺-depleted BG11 without NaCl. To induce ectopic IsaR1 expression in IsaR1OE, all cultures were supplemented with 2 µM

Cu²⁺; then, after 24 h, a sudden increase in salinity was provoked by adding crystalline NaCl to a final concentration of 4%. In the WT strain, the GgpS protein strongly accumulated 4 h after salt shock (**Figure 3A**). In the IsaR1OE strain, however, GgpS accumulation was clearly delayed compared to the WT strain (**Figure 3A**). In IsaR1OE cells that were cultivated for 7 days in the presence of 4% NaCl and could thus be considered salt-acclimated, the GgpS abundance remained more than 50% lower compared to the WT (**Figure 3B**), demonstrating that IsaR1 overexpression also has a strong effect on the steady-state abundance of GgpS. However, since the experimental setup using high, ectopic IsaR1 expression has a rather artificial character we were wondering if such a dynamic expression response might also be observable for the chromosomal copy of the *isaR1* gene at high salinity. We performed similar salt shock experiments using the WT strain. Indeed, in response to salt stress IsaR1 showed increased expression and highly dynamic kinetics similar to *ggpS* (**Figure 3C**). Altogether, the data indicate that IsaR1 interferes with *ggpS* expression after salt shock and delays the *de novo* synthesis of the key enzyme of GG synthesis.

IsaR1 overexpression results in slower GG accumulation after salt shock.

All previous results suggested that IsaR1 interacts with the *ggpS* mRNA and is involved in controlling the *de novo* synthesis of GgpS. Assuming that the reaction catalyzed by GgpS is the rate-limiting step, the delayed GgpS synthesis observed in the IsaR1OE strain should also result in a decreased accumulation rate of GG upon salt shock. It was previously shown that under freshwater conditions, cells are virtually free of GG but that GG quickly accumulates within the first few hours after salt shock (Erdmann *et al.*, 1992) by activating preformed GgpS enzyme and inducing its expression in a salinity-dependent manner (Marin *et al.*, 2002). It has been shown that modulating the preformed GgpS levels also changed the rate of GG synthesis upon salt shock (Klähn *et al.*, 2010). To verify an impact of IsaR1 on GG accumulation, we again performed salt shock experiments and measured the internal GG amounts in the IsaR1OE and WT strains at different time points. Indeed, within the first few hours after salt shock, the IsaR1OE strain showed a lowered rate of GG accumulation

compared to the WT strain (**Figure 4A**). However, this effect was observed only transiently. In salt-acclimated cells, the GG levels were similar in both strains (**Figure 4B**), although the GgpS protein level was decreased in the IsaR1OE strain. Thus, the impact of IsaR1 on GG synthesis is restricted to the initial phase after the shift in salinity. Nevertheless, consistent with a decreased GG accumulation rate in the IsaR1OE strain, this strain also showed altered kinetics of the secondary compatible solute, sucrose (Suc) (**Figure 4C**). In the IsaR1OE strain, the initial Suc accumulation after salt shock was similar to the WT strain, but the maximum amount was reached a few hours later (**Figure 4C**). The shift of the maximum Suc level was observed in the same time range in which a difference in GG synthesis was seen, indicating that the decreased levels of GG at this time caused a feedback in the Suc pool and elongated its transient accumulation. After 48 h, the Suc levels were similar in both strains as observed before for GG. Moreover, in salt-acclimated IsaR1OE cells, we observed an increase in the G3P pool (**Figure 4D**) that serves as a precursor for GG synthesis. This finding is consistent with a decreased GG synthesis rate, although the final GG levels were similar in all tested strains. Apparently, the steady-state GG amounts are not determined by the overall GgpS amount as after salt shock. It has been shown that GgpS activity is regulated at the biochemical level due to binding and/or releasing the protein from the inhibitory binding of DNA in an ion-content dependent manner (Novak *et al.*, 2011). This biochemical regulation primarily ensures the stress-proportional accumulation of GG in long-term acclimated cells.

The *ggpS* gene is responsive to iron limitation via post-transcriptional regulation by IsaR1.

In the previous experiments we focused on the effect ectopic IsaR1 expression has on the salt-inducible expression of *ggpS* and GG biosynthesis. Albeit the highly stimulated IsaR1 expression in WT during salt shock this effect appears to be transient (**Figure 3C**). However, IsaR1 has been shown to be strongly and continuously induced under iron limitation and the core set of verified IsaR1 target genes is also iron-regulated (Georg *et al.*, 2017). Because the *ggpS* mRNA abundance is strongly decreased upon IsaR1 overexpression, an up-

regulation of IsaR1 by iron-depletion in the WT strain might also interfere with *ggsS*, thus making it iron-responsive. To test this hypothesis, *ggsS* gene expression was analyzed in iron-depleted cells of the WT, IsaR1OE and in addition an *isaR1* deletion strain, which was also obtained in a previous study (Georg *et al.*, 2017). To ensure adequate *ggsS* expression, all strains were grown in salt-supplemented BG11 medium (4% NaCl), and iron limitation was induced by the addition of the Fe²⁺-specific chelator desferrioxamine B (DFB). After long-term iron-depletion, the *ggsS* mRNA levels were similar in all strains (**Figure 5A**). In contrast, the Δ *isaR1* knockout strain showed increased levels of the GgsS protein, even after 7 days of iron depletion, indicating that IsaR1 is also involved in maintaining the appropriate GgsS levels in iron-limited cells (**Figure 5B**). The conclusion that the *ggsS* gene is indeed iron-regulated was further supported by measuring expression kinetics after the addition of DFB to the WT and Δ *isaR1* cultures (**Figure 6**). In WT, the IsaR1 levels started to increase strongly two days after the depletion of Fe²⁺. At the same time, the *ggsS* mRNA levels dropped by ~40% compared to the initial levels (**Figure 6A**). In addition, the GgsS protein levels also decreased upon iron depletion (**Figure 6B**). As expected, no IsaR1 was detectable in the Δ *isaR1* mutant. Interestingly, the *ggsS* mRNA level also decreased in this strain, albeit at a slightly lower rate than in the WT strain. However, the GgsS protein level did not decrease in the Δ *isaR1* mutant upon iron limitation, in contrast to the WT strain (**Figure 6B**). These data support the idea that the *ggsS* gene is both salt-regulated and iron-regulated, the latter of which is at least partially mediated by IsaR1.

Discussion

Severe iron starvation and osmotic shock are both challenging stresses for microorganisms. Using IsaR1 overexpression and knockout strains we observed an inverse relationship between IsaR1 abundance and *ggsS* expression levels through various experiments, suggesting that the responses to these two stresses become coordinated through the action of IsaR1 on the 5'UTR of *ggsS*. Such an integrating function highlights the possible

importance of small regulatory RNAs as fine tuners of gene expression under combined stress conditions, which likely also applies to other sRNA regulators in bacteria.

Since IsaR1 is a widely conserved post-transcriptional regulator of iron homeostasis among cyanobacteria (Georg *et al.*, 2017) the interconnection with a salt acclimation mechanism is somewhat surprising. However, we showed that IsaR1 expression is highly dynamic in response to fluctuations in external iron supply and salinity as well (**Figures 3 and 6**) enabling the possibility of posttranscriptional regulation of the salt-induced *ggpS* gene by IsaR1. The interaction of IsaR1 with the *ggpS* mRNA impacts the biosynthesis of GgpS and GG upon salt shock in *Synechocystis*, which might also occur in other cyanobacteria expressing the two genes. Although only some cyanobacterial genomes harbor homologs of both *ggpS* and *isaR1*, *in silico* analyses have suggested that this type of regulation might also be common in other salt-tolerant cyanobacteria, such as *Halotheca* sp. PCC 7418 (**Supplementary Figure S2**).

Consistent with a lowered *de novo* GgpS synthesis and reduced GG accumulation rate upon salt shock, IsaR1 overexpression also affected the pool of the secondary compatible solute Suc (**Figure 4C**). Suc is known to accumulate more rapidly than GG after a salt shock but declines in concentration, when GG accumulates in later phases of the salt-acclimation process (Reed *et al.*, 1985). Probably this is due to its replacement by GG, since internal GG and Suc accumulation seem to be synchronized. That both osmolytes can partially be replaced by each other is supported by the fact that a $\Delta ggpS$ mutant strain accumulated increased amounts of sucrose instead of GG (Marin *et al.*, 1998). The change of Suc accumulation in parallel to the decreased GG accumulation rate in response to IsaR1 overexpression supports our conclusion that IsaR1 indeed interferes with the salt acclimation process in *Synechocystis*. This is in addition to its primary regulatory function in the iron-dependent regulation of photosynthetic apparatus proteins (Georg *et al.*, 2017).

However, the modulation of IsaR1 expression did not alter the steady-state GG levels in long-term salt-acclimated cells. Clearly, the IsaR1-mediated regulation of *ggpS* is not an

'on/off' mechanism but fine-tunes the rate of GgpS synthesis according to environmental conditions. Such regulation might be particularly useful under fluctuating salt concentrations, such as in estuary brackish water habitats, where an increase in salinity is accompanied by a rapid removal of iron from river water (Boyle *et al.*, 1977). Thus, in addition to salinity changes, estuary habitats exhibit strong fluctuations in iron availability. Moreover, the availability of iron in ocean waters is predominately limited by its solubility (Johnson *et al.*, 1997; Liu and Millero, 2002). Consistently, iron is the major limiting factor for phytoplankton growth in many marine habitats (Boyd *et al.*, 2007; Moore *et al.*, 2013). Therefore, the co-regulation of iron and salt acclimation is potentially beneficial for bacteria living predominantly under such conditions. Interestingly, it has been shown that high salinity also causes iron limitation in *Bacillus subtilis*, which triggers the de-repression of a variety of iron-controlled genes (Hoffmann *et al.*, 2002; Steil *et al.*, 2003). In *Synechocystis*, the *isiA* gene, which encodes a chlorophyll-binding protein, is strongly up-regulated under iron limitation but was also shown to respond to salt stress (Vinnemeier *et al.*, 1998). As mentioned, we found that IsaR1 expression is also highly stimulated upon salt shock and shows expression kinetics similar to *ggpS* (**Figure 3**). However, it is not yet clear whether this is a direct salinity effect on IsaR1 expression or is indirectly caused by lowered iron availability.

In addition to the effects IsaR1 overexpression has on the acclimation to increasing salinity, we show that *ggpS* expression is also down-regulated in response to iron limitation. This has probably been overseen so far, since previous analyses investigating the iron starvation response were performed in low-salt medium, a condition at which *ggpS* is only weakly expressed (Hernández-Prieto *et al.*, 2012). Since an *isaR1* knockout strain is impaired in *ggpS* downregulation under iron limitation, IsaR1 is involved in that regulation. At a first glance, the biological significance of an IsaR1-mediated down-regulation of *ggpS* expression under iron limitation might not seem obvious since GG synthesis is not iron-dependent per se. However, high level GG accumulation requires substantial quantities of energy and metabolic resources, which are products of iron dependent pathways. This is obvious for ATP production because photosynthetic and respiratory complexes are rich in iron-cofactors.

In addition, GgpS competes with other enzymatic reactions for the precursors. For example, ADP-glucose is also the glucosyl donor for cyanobacterial glycogen synthesis (Ball and Morell, 2003). It was reported that iron limitation causes a large increase in glycogen storage granules in the freshwater cyanobacterium *Synechococcus elongatus* PCC 7942 (Sherman and Sherman, 1983) (synonymous with *Anacystis nidulans* R2). Assuming that a similar increase in glycogen also occurs under iron limitation in other cyanobacteria, diminishing ADP-glucose consumption by GgpS might be beneficial in *Synechocystis*.

The second GgpS substrate, G3P, is also used in high quantities for the *de novo* synthesis of membrane lipids. It is well-known that stress acclimation of bacterial cells often includes an adjustment of the fatty acid (FA) composition in the membrane to modify its biophysical properties (Mansilla *et al.*, 2004; Zhang and Rock, 2008). Interestingly, changes in the fatty acid composition have been reported for cyanobacteria under iron deficiency (Ivanov *et al.*, 2007) and high salinities (Allakhverdiev *et al.*, 1999, 2001). Sudden FA modification on existing membranes is mainly performed by FA desaturases that catalyze O₂-dependent dehydrogenations and use iron as a co-factor (Fox *et al.*, 1993; Shanklin *et al.*, 2009). Hence, it is likely that FA desaturase activities are affected under iron-limitation. At high salinity, however, FA unsaturation is required in cyanobacteria (Allakhverdiev *et al.*, 1999). It could be speculated that at high salinity and parallel iron limitation, cells increase *de novo* synthesis of unsaturated FAs that are incorporated into the membrane. However, such a process would compete with GG synthesis for the G3P pool, which might become limiting.

An additional hint towards a limiting G3P pool, is the presence of three independent G3P-synthesizing enzymes in *Synechocystis*. According to CyanoExpress (Hernandez-Prieto and Futschik, 2012), the gene *slr1755*, which encodes the NAD⁺-dependent G3P dehydrogenase, is constitutively expressed. However, the two other genes, a glycerol kinase (*glpK*, *slr1672*) and a second G3P dehydrogenase (*glpD*, *slr1085*), are strongly up-regulated under salt stress (Marin *et al.*, 2004). The up-regulation of two G3P synthesizing enzymes supports the idea that G3P is a limiting precursor during high salt conditions and that its consumption

could be fine-tuned by IsaR1 during parallel iron starvation. Consistently, we showed that changes in IsaR1 expression indeed affect the G3P pool at high salinity (**Figure 4D**). Nevertheless, the here suggested connection is highly speculative and a physiological meaning of an iron-dependent *ggpS* expression remains to be elucidated in future analyses.

Experimental Procedures

Strains and growth conditions

Synechocystis sp. PCC 6803, substrain “PCC-M” (Trautmann *et al.*, 2012), served as the WT strain. The IsaR1 mutant strains were previously described (Georg *et al.*, 2017). Liquid cultures were grown with gentle agitation in Cu²⁺-free BG11 medium (Rippka *et al.*, 1979) buffered with 20 mM TES, pH 8.0 at 30°C under continuous white light illumination of 50 $\mu\text{mol quanta m}^{-2} \text{ s}^{-1}$. To induce the ectopic expression of IsaR1 driven by the *petE* promoter in strain IsaR1OE, 2 μM CuSO₄ was added to all cultures. To induce salt stress, crystalline, autoclaved NaCl was added at a final concentration of 4% (m/v). To induce iron starvation, the iron chelator desferrioxamine B (DFB, Sigma-Aldrich, USA) was added at a final concentration of 300 μM , which was 10-fold higher than the iron amount in BG11.

RNA extraction and Northern blots

RNA extraction and Northern hybridization with ³²P-labelled, single-stranded transcript probes was carried out as previously described (Steglich *et al.*, 2008; Hein *et al.*, 2013). The primers used to amplify templates for generating RNA probes by *in vitro* transcription are given in **Supplementary Table S1**.

Protein extraction and immunoblots

Cells were mechanically disrupted as described (Baumgartner *et al.*, 2016). The protein extract was fractionated by SDS-PAGE on a 15% gel and blotted onto nitrocellulose membranes (AmershamTM ProtranTM Premium 0.45 μm , GE Healthcare, USA) by semi-dry electrophoretic transfer. Prior to immunohybridization were blocked with 5% milk powder in TBS-T and hybridized with rabbit serum containing anti-GgpS primary antibody (titer 1:5,000)

(Marin *et al.*, 2002). All washing steps were performed with gentle agitation in TBS-T at room temperature. An HRP-conjugated anti-rabbit secondary antibody and the ECL start Western Blotting Detection Reagent (GE Healthcare, USA) were used to detect anti-GgpS. Densitometric evaluation was performed using Quantity One software (BIO-RAD, USA).

GFP reporter assays

For the experimental target verification, we used a previously described reporter system (Urban and Vogel, 2007; Corcoran *et al.*, 2012). The primers used for cloning and the resulting plasmids are given in **Supplementary Tables S1** and **S2**. pZE12_IsaR1_WT was generated by amplifying the backbone of pZE12-luc using the primers PLLacoB and PLLacoD and IsaR1 from *Synechocystis* gDNA using the primers Syr22_5_phos and Syr22_3_xbaI. Both PCR products were digested with *Xba*I and ligated. pXG10_ggpS_WT was generated by amplifying the entire *ggpS* 5'UTR (from +1 to +435, where +1 refers to the first transcribed nucleotide; the first nucleotide of start codon is at pos. +379) from gDNA using the primers ggpS_5_PCC6803_NsiI and ggpS_3_PCC6803_NheI followed by a *Nsi*I/*Nhe*I digestion and subsequent ligation with pXG10_SF. Point mutations within the *ggpS* and IsaR1 sequences were introduced by PCR amplification of the original plasmids pXG10_ggpS_WT or pZE12_IsaR1_WT by using primer combinations ggpS_mut_5/ggpS_mut_3 and IsaR1_gg_mut_5/IsaR1_gg_mut_3, respectively. The PCR products were purified using the NucleoSpin Gel and PCR Clean Up kit (Macherey-Nagel, Germany) and enzymatically digested with *Dpn*I at 37°C. *E. coli* DH5α cells were transformed with the final plasmids, which were subsequently checked by sequencing. For target verification, *E. coli* TOP10 cells were transformed with seven different combinations of plasmids (pXG0 + pJV300; pXG10_ggpS_WT + pJV300; pXG10_ggpS_mut + pJV300; pXG10_ggpS_WT + pZE12_IsaR1_WT; pXG10_ggpS_WT + pZE12_IsaR1_mut; pXG10_ggpS_mut + pZE12_IsaR1_WT; pXG10_ggpS_mut + pZE12_IsaR1_mut). The plasmids pXG0 and pJV300 served as negative controls. For the flow cytometry-based fluorescence measurements were performed as described (Wright *et al.*, 2013).

Glucosylglycerol quantification

Low molecular mass carbohydrates were extracted and determined using gas chromatography as previously described (Hagemann *et al.*, 2008; Klähn *et al.*, 2010).

Glycerol-3-phosphate measurements

G3P was determined using an established gas chromatography-electron ionization-time-of-flight-mass spectrometry (GC-EI-TOF-MS) profiling platform as described (Kopka *et al.*, 2017). Relative metabolite levels were measured in arbitrary units. Average percentages relative to the maximum measurement and standard deviations were calculated after outlier removal.

Acknowledgements

We thank Dr. Jens Georg and Sarah Pick for initial cloning of the pXG10_ggpS_WT plasmid, Joke Lambrecht for his advice in flow cytometry and Manja Henneberg for technical assistance during GC measurements.

Conflict of Interest

The authors declare no competing financial interests.

References

- Allakhverdiev, S.I., Kinoshita, M., Inaba, M., Suzuki, I., and Murata, N. (2001) Unsaturated fatty acids in membrane lipids protect the photosynthetic machinery against salt-induced damage in *Synechococcus*. *Plant Physiol.* **125**: 1842–1853.
- Allakhverdiev, S.I., Nishiyama, Y., Suzuki, I., Tasaka, Y., and Murata, N. (1999) Genetic engineering of the unsaturation of fatty acids in membrane lipids alters the tolerance of *Synechocystis* to salt stress. *Proc Natl Acad Sci U S A* **96**: 5862–5867.
- Andrews, S.C., Robinson, A.K., and Rodríguez-Quiriones, F. (2003) Bacterial iron homeostasis. *FEMS Microbiol. Rev.* **27**: 215–237.
- Ball, S.G. and Morell, M.K. (2003) From bacterial glycogen to starch: understanding the biogenesis of the plant starch granule. *Annu Rev Plant Biol* **54**: 207–233.
- Baumgartner, D., Kopf, M., Klähn, S., Steglich, C., and Hess, W.R. (2016) Small proteins in cyanobacteria provide a paradigm for the functional analysis of the bacterial microproteome. *BMC Microbiol.* **16**: 285.
- Boyd, P.W., Jickells, T., Law, C.S., Blain, S., Boyle, E.A., Buesseler, K.O., et al. (2007) Mesoscale iron enrichment experiments 1993-2005: synthesis and future directions. *Science* **315**: 612–617.
- Boyle, E.A., Edmond, J.M., and Sholkovitz, E.R. (1977) The mechanism of iron removal in estuaries. *Geochimica et Cosmochimica Acta* **41**: 1313–1324.
- Brown, A.D. (1976) Microbial water stress. *Bacteriol Rev* **40**: 803–846.
- Busch, A., Richter, A.S., and Backofen, R. (2008) IntaRNA: efficient prediction of bacterial sRNA targets incorporating target site accessibility and seed regions. *Bioinformatics* **24**: 2849–2856.
- Caron, M.-P., Lafontaine, D.A., and Massé, E. (2010) Small RNA-mediated regulation at the level of transcript stability. *RNA Biol* **7**: 140–144.
- Corcoran, C.P., Podkaminski, D., Papenfort, K., Urban, J.H., Hinton, J.C.D., and Vogel, J. (2012) Superfolder GFP reporters validate diverse new mRNA targets of the classic porin regulator, MicF RNA. *Mol. Microbiol.* **84**: 428–445.
- Englund, E., Liang, F., and Lindberg, P. (2016) Evaluation of promoters and ribosome binding sites for biotechnological applications in the unicellular cyanobacterium *Synechocystis* sp. PCC 6803. *Sci Rep* **6**.
- Erdmann, N., Fulda, S., and Hagemann, M. (1992) Glucosylglycerol accumulation during salt acclimation of two unicellular cyanobacteria. *J Gen Microbiol* **138**: 363–368.
- Fox, B.G., Shanklin, J., Somerville, C., and Münck, E. (1993) Stearoyl-acyl carrier protein delta 9 desaturase from *Ricinus communis* is a diiron-oxo protein. *Proc Natl Acad Sci U S A* **90**: 2486–2490.
- Georg, J., Dienst, D., Schürgers, N., Wallner, T., Kopp, D., Stazic, D., et al. (2014) The small regulatory RNA SyR1/PsrR1 controls photosynthetic functions in cyanobacteria. *Plant Cell* **26**: 3661–3679.
- Georg, J., Kostova, G., Vuorijoki, L., Schön, V., Kadowaki, T., Huokko, T., et al. (2017) Acclimation of oxygenic photosynthesis to iron starvation is controlled by the sRNA IsaR1. *Curr. Biol.* **27**: 1425–1436.
- Ghassemian, M., Wong, B., Ferreira, F., Markley, J.L., and Straus, N.A. (1994) Cloning, sequencing and transcriptional studies of the genes for cytochrome c-553 and plastocyanin from *Anabaena* sp. PCC 7120. *Microbiology (Reading, Engl.)* **140** (Pt 5): 1151–1159.
- Hagemann, M. (2011) Molecular biology of cyanobacterial salt acclimation. *FEMS Microbiol. Rev.* **35**: 87–123.
- Hagemann, M. and Erdmann, N. (1994) Activation and pathway of glucosylglycerol synthesis in the cyanobacterium *Synechocystis* sp. PCC 6803. *Microbiology* **140**: 1427–1431.
- Hagemann, M., Ribbeck-Busch, K., Klähn, S., Hasse, D., Steinbruch, R., and Berg, G. (2008) The plant-associated bacterium *Stenotrophomonas rhizophila* expresses a new enzyme for the synthesis of the compatible solute glucosylglycerol. *J. Bacteriol.* **190**: 5898–5906.

- Halliwell, B. and Gutteridge, J.M. (1992) Biologically relevant metal ion-dependent hydroxyl radical generation. An update. *FEBS Lett.* **307**: 108–112.
- Hantke, K. (2001) Iron and metal regulation in bacteria. *Curr. Opin. Microbiol.* **4**: 172–177.
- Hein, S., Scholz, I., Voß, B., and Hess, W.R. (2013) Adaptation and modification of three CRISPR loci in two closely related cyanobacteria. *RNA Biol.* **10**: 852–864.
- Hernandez-Prieto, M.A. and Futschik, M.E. (2012) CyanoEXpress: A web database for exploration and visualisation of the integrated transcriptome of cyanobacterium *Synechocystis* sp. PCC6803. *Bioinformatics* **8**: 634–638.
- Hernández-Prieto, M.A., Schön, V., Georg, J., Barreira, L., Varela, J., Hess, W.R., and Futschik, M.E. (2012) Iron Deprivation in *Synechocystis*: Inference of Pathways, Non-coding RNAs, and Regulatory Elements from Comprehensive Expression Profiling. *G3 (Bethesda)* **2**: 1475–1495.
- Hoffmann, T., Schütz, A., Brosius, M., Völker, A., Völker, U., and Bremer, E. (2002) High-Salinity-Induced Iron Limitation in *Bacillus subtilis*. *J Bacteriol* **184**: 718–727.
- Ivanov, A.G., Krol, M., Selstam, E., Sane, P.V., Sveshnikov, D., Park, Y.-I., et al. (2007) The induction of CP43' by iron-stress in *Synechococcus* sp. PCC 7942 is associated with carotenoid accumulation and enhanced fatty acid unsaturation. *Biochim. Biophys. Acta* **1767**: 807–813.
- Johnson, K.S., Gordon, R.M., and Coale, K.H. (1997) What controls dissolved iron concentrations in the world ocean? *Marine Chemistry* **57**: 137–161.
- Kempf, B. and Bremer, E. (1998) Uptake and synthesis of compatible solutes as microbial stress responses to high-osmolality environments. *Arch Microbiol* **170**: 319–330.
- Kizawa, A., Kawahara, A., Takimura, Y., Nishiyama, Y., and Hihara, Y. (2016) RNA-seq Profiling Reveals Novel Target Genes of LexA in the Cyanobacterium *Synechocystis* sp. PCC 6803. *Front Microbiol* **7**: 193.
- Klähn, S., Höhne, A., Simon, E., and Hagemann, M. (2010) The gene *ssl3076* encodes a protein mediating the salt-induced expression of *ggpS* for the biosynthesis of the compatible solute glucosylglycerol in *Synechocystis* sp. strain PCC 6803. *J. Bacteriol.* **192**: 4403–4412.
- Klähn, S., Schaal, C., Georg, J., Baumgartner, D., Knippen, G., Hagemann, M., et al. (2015) The sRNA NsiR4 is involved in nitrogen assimilation control in cyanobacteria by targeting glutamine synthetase inactivating factor IF7. *Proc. Natl. Acad. Sci. U.S.A.* **112**: E6243-52.
- Kopka, J., Schmidt, S., Dethloff, F., Pade, N., Berendt, S., Schottkowski, M., et al. (2017) Systems analysis of ethanol production in the genetically engineered cyanobacterium *Synechococcus* sp. PCC 7002. *Biotechnol Biofuels* **10**: 56.
- Lebre, P.H., De Maayer, P., and Cowan, D.A. (2017) Xerotolerant bacteria: surviving through a dry spell. *Nat. Rev. Microbiol.* **15**: 285–296.
- Liu, X. and Millero, F.J. (2002) The solubility of iron in seawater. *Marine Chemistry* **77**: 43–54.
- Mansilla, M.C., Cybulski, L.E., Albanesi, D., and de Mendoza, D. (2004) Control of membrane lipid fluidity by molecular thermosensors. *J. Bacteriol.* **186**: 6681–6688.
- Marin, K., Huckauf, J., Fulda, S., and Hagemann, M. (2002) Salt-dependent expression of glucosylglycerol-phosphate synthase, involved in osmolyte synthesis in the cyanobacterium *Synechocystis* sp. strain PCC 6803. *J. Bacteriol.* **184**: 2870–2877.
- Marin, K., Kanesaki, Y., Los, D.A., Murata, N., Suzuki, I., and Hagemann, M. (2004) Gene expression profiling reflects physiological processes in salt acclimation of *Synechocystis* sp. strain PCC 6803. *Plant Physiol.* **136**: 3290–3300.
- Marin, K., Zuther, E., Kerstan, T., Kunert, A., and Hagemann, M. (1998) The *ggpS* gene from *Synechocystis* sp. strain PCC 6803 encoding glucosyl-glycerol-phosphate synthase is involved in osmolyte synthesis. *J. Bacteriol.* **180**: 4843–4849.
- Massé, E. and Gottesman, S. (2002) A small RNA regulates the expression of genes involved in iron metabolism in *Escherichia coli*. *Proc. Natl. Acad. Sci. U.S.A.* **99**: 4620–4625.

- Miao, X., Wu, Q., Wu, G., and Zhao, N. (2003) Sucrose accumulation in salt-stressed cells of *agp* gene deletion-mutant in cyanobacterium *Synechocystis* sp. PCC 6803. *FEMS Microbiol. Lett.* **218**: 71–77.
- Moore, C.M., Mills, M.M., Arrigo, K.R., Berman-Frank, I., Bopp, L., Boyd, P.W., et al. (2013) Processes and patterns of oceanic nutrient limitation. *Nature Geosci* **6**: 701–710.
- Novak, J.F., Stirnberg, M., Roenneke, B., and Marin, K. (2011) A novel mechanism of osmosensing, a salt-dependent protein-nucleic acid interaction in the cyanobacterium *Synechocystis* Species PCC 6803. *J. Biol. Chem.* **286**: 3235–3241.
- Reed, R.H. and Stewart, W.D.P. (1985) Osmotic adjustment and organic solute accumulation in unicellular cyanobacteria from freshwater and marine habitats. *Mar. Biol.* **88**: 1–9.
- Reed, R.H., Warr, S.R.C., Richardson, D.L., Moore, D.J., and Stewart, W.D.P. (1985) Multiphasic osmotic adjustment in a euryhaline cyanobacterium. *FEMS Microbiology Letters* **28**: 225–229.
- Rippka, R., Deruelles, J., Waterbury, J.B., Herdman, M., and Stanier, R.Y. (1979) Generic assignments, strain histories and properties of pure cultures of cyanobacteria. *J. Gen. Microbiol.* **111**: 1–61.
- Shanklin, J., Guy, J.E., Mishra, G., and Lindqvist, Y. (2009) Desaturases: emerging models for understanding functional diversification of diiron-containing enzymes. *J. Biol. Chem.* **284**: 18559–18563.
- Sherman, D.M. and Sherman, L.A. (1983) Effect of iron deficiency and iron restoration on ultrastructure of *Anacystis nidulans*. *J. Bacteriol* **156**: 393–401.
- Stanier, R.Y., Kunisawa, R., Mandel, M., and Cohen-Bazire, G. (1971) Purification and properties of unicellular blue-green algae (order Chroococcales). *Bacteriol Rev* **35**: 171–205.
- Steglich, C., Futschik, M.E., Lindell, D., Voss, B., Chisholm, S.W., and Hess, W.R. (2008) The challenge of regulation in a minimal photoautotroph: non-coding RNAs in *Prochlorococcus*. *PLoS Genet.* **4**: e1000173.
- Steil, L., Hoffmann, T., Budde, I., Völker, U., and Bremer, E. (2003) Genome-wide transcriptional profiling analysis of adaptation of *Bacillus subtilis* to high salinity. *J. Bacteriol.* **185**: 6358–6370.
- Storz, G., Vogel, J., and Wassarman, K.M. (2011) Regulation by small RNAs in bacteria: expanding frontiers. *Mol. Cell* **43**: 880–891.
- Tan, X., Yao, L., Gao, Q., Wang, W., Qi, F., and Lu, X. (2011) Photosynthesis driven conversion of carbon dioxide to fatty alcohols and hydrocarbons in cyanobacteria. *Metab. Eng.* **13**: 169–176.
- Trautmann, D., Voss, B., Wilde, A., Al-Babili, S., and Hess, W.R. (2012) Microevolution in cyanobacteria: re-sequencing a motile substrain of *Synechocystis* sp. PCC 6803. *DNA Res.* **19**: 435–448.
- Urban, J.H. and Vogel, J. (2007) Translational control and target recognition by *Escherichia coli* small RNAs *in vivo*. *Nucleic Acids Res* **35**: 1018–1037.
- Vinnemeier, J., Kunert, A., and Hagemann, M. (1998) Transcriptional analysis of the *isiAB* operon in salt-stressed cells of the cyanobacterium *Synechocystis* sp. PCC 6803. *FEMS Microbiol. Lett.* **169**: 323–330.
- Wandersman, C. and Delepelaire, P. (2004) Bacterial iron sources: from siderophores to hemophores. *Annu. Rev. Microbiol.* **58**: 611–647.
- Waters, L.S. and Storz, G. (2009) Regulatory RNAs in bacteria. *Cell* **136**: 615–628.
- Wilderman, P.J., Sowa, N.A., FitzGerald, D.J., FitzGerald, P.C., Gottesman, S., Ochsner, U.A., and Vasil, M.L. (2004) Identification of tandem duplicate regulatory small RNAs in *Pseudomonas aeruginosa* involved in iron homeostasis. *Proc. Natl. Acad. Sci. U.S.A.* **101**: 9792–9797.
- Wood, J.M., Bremer, E., Csonka, L.N., Kraemer, R., Poolman, B., van der Heide, T., and Smith, L.T. (2001) Osmosensing and osmoregulatory compatible solute accumulation by bacteria. *Comp. Biochem. Physiol., Part A Mol. Integr. Physiol.* **130**: 437–460.
- Wright, P.R., Georg, J., Mann, M., Sorescu, D.A., Richter, A.S., Lott, S., et al. (2014) CopraRNA and IntaRNA: predicting small RNA targets, networks and interaction domains. *Nucleic Acids Res.* **42**: W119–123.

- Wright, P.R., Richter, A.S., Papenfort, K., Mann, M., Vogel, J., Hess, W.R., et al. (2013) Comparative genomics boosts target prediction for bacterial small RNAs. *Proc. Natl. Acad. Sci. U.S.A.* **110**: E3487-3496.
- Zhang, Y.-M. and Rock, C.O. (2008) Membrane lipid homeostasis in bacteria. *Nat. Rev. Microbiol.* **6**: 222–233.

Figure legends

Figure 1. Changes in the *ggpS* mRNA and GgpS protein abundances in response to altered *IsaR1* expression. **A:** Northern blots showing the RNA levels of *ggpS* and *IsaR1* in cells grown in Cu^{2+} -depleted BG11 or 24 h after the addition of $2\ \mu\text{M}\ \text{Cu}^{2+}$ to induce the *petE* promoter driven expression of *IsaR1*. The blots were hybridized with ^{32}P -labeled, single-stranded RNA probes. To ensure adequate *ggpS* expression, all strains were cultivated in presence of 4% (w/v) NaCl throughout the experiment. **B:** GgpS protein levels 24 h after the addition of Cu^{2+} . L.c. – loading control, either excerpts of the corresponding ethidium bromide stained RNA gels showing the 16S rRNA (Northern blots) or an excerpt of a Ponceau-stained membrane showing the same size range of proteins (immunoblots). For each strain, two replicates are shown (1 and 2). **C:** Densitometric evaluation of the signals shown in panels a and b after normalization to the loading control. The values for each strain are indicated as relative levels referring to WT (replicate 1) and are given as the means \pm SD for the two replicates. WT, *Synechocystis* wild type carrying an empty pVZ322-*PpetE::oop* plasmid backbone; *IsaR1OE*, strain carrying pVZ322-*PpetE::isaR1::oop* plasmid (overexpression strain).

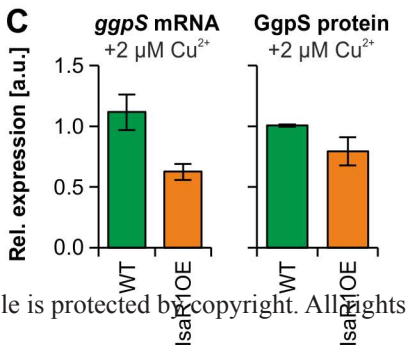
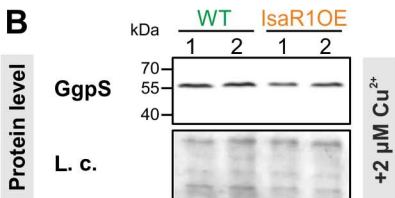
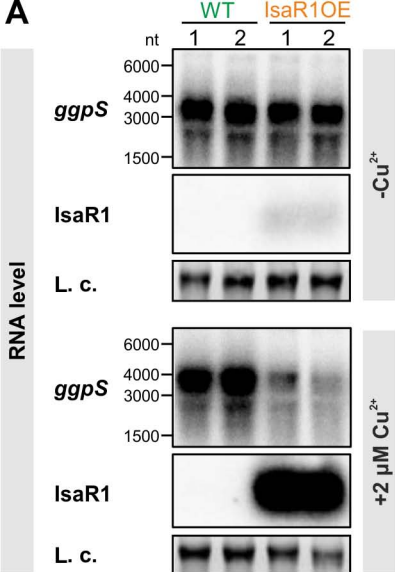
Figure 2. Verification of the post-transcriptional regulation of *ggpS* through direct *IsaR1* interaction using a GFP reporter system. **A+B:** Predicted interaction site between *IsaR1* and the *ggpS* 5'UTR close to the *ggpS* start codon (boxed) using the respective WT sequences (**A**) and sequences carrying complementary point mutations at pos. +19 (*IsaR1*, G to C) and pos. +354 (*ggpS*, C to G), respectively (**B**). We chose mutations within the seed region (underlined) that drastically reduced the hybridization energies but did not change the secondary structure of the RNAs. Predictions were made using the IntaRNA webserver (Busch *et al.*, 2008) with default parameters. In the RNA sequences, the numbers refer to the transcriptional start site (TSS) at position +1. **C:** GFP fluorescence measurements of *E. coli* TOP10 strains with various combinations of plasmids expressing *IsaR1* and the *sgfp* gene fused to the 5'UTR of *ggpS*. The plasmids pXG-0 (encoding luciferase) and pJV300 (encoding a control RNA) were used as negative controls. **D:** Analogous data presented as fold repressions for various combinations, including plasmids expressing the point mutated sequences. Representative fluorescence data are given as the means \pm SD of six biological replicates from two independent experiments. Asterisks indicate significant differences determined by *t* test (***, $P < 0.001$).

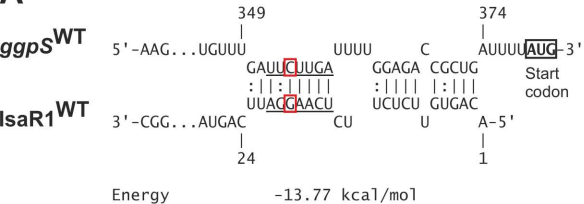
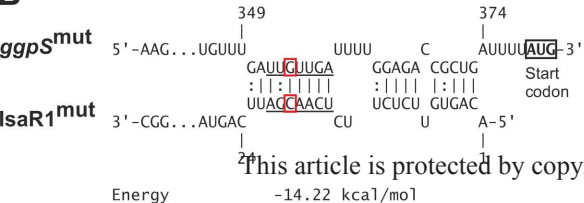
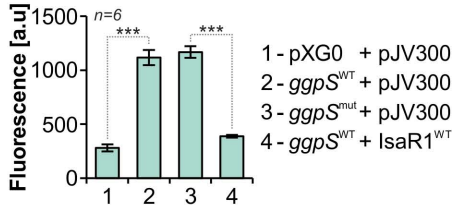
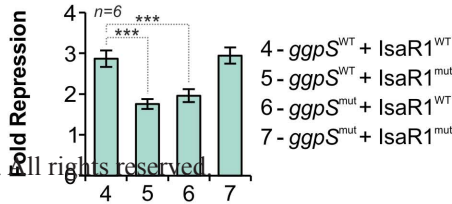
Figure 3. Effect of altered *IsaR1* expression on *de novo* GgpS synthesis. **A:** A Western blot that was hybridized with a GgpS-specific antibody and shows its expression kinetics in the *IsaR1* mutant strains in response to a sudden salt shock. Ponceau-stained parts of the corresponding membranes are shown as the loading control (L.c.). Prior to salt shock which was triggered by adding crystalline NaCl to a final concentration of 4% (w/v), overexpression of *IsaR1* was induced with $2\ \mu\text{M}\ \text{Cu}^{2+}$ for 24 h. It should be noted that the samples for the WT and *IsaR1OE* were loaded onto the same membrane and thus kinetics are directly comparable. **B:** Steady-state GgpS protein levels in long-term salt acclimated cells. The same experimental setup was used as in panel **A** but protein samples were taken 7 days after salt shock. For each strain, two replicates are shown (1 and 2). WT, *Synechocystis* wild type carrying an empty pVZ322-*PpetE::oop* plasmid backbone; *IsaR1OE*, strain carrying pVZ322-*PpetE::isaR1::oop* plasmid (overexpression strain). **C:** Northern blot using *ggpS* or *IsaR1* specific radio-labelled probes showing expression kinetics of both RNAs upon salt shock (4% NaCl) in WT.

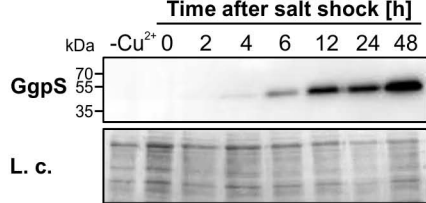
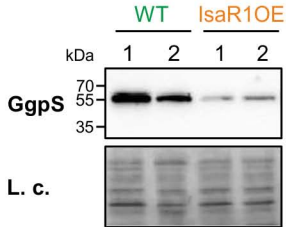
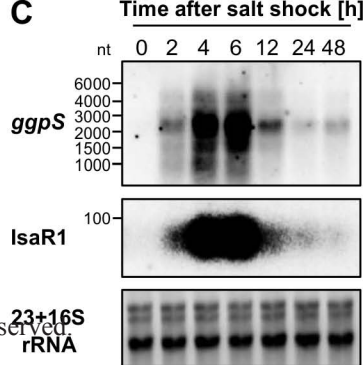
Figure 4. Intracellular accumulation of glucosylglycerol (GG) and the secondary compatible solute sucrose (Suc) after salt shock and the levels of glycerol 3-phosphate (G3P) under combined salt and iron-stress. **A:** GG accumulation kinetics during the first hours after sudden salt shock of 4% (w/v) NaCl in a representative culture of the WT and the overexpression strain IsaR1OE. The experiment was performed twice using two biological replicates, respectively, and albeit different ranges in all cases lower GG accumulation rates were observed in IsaR1OE. **B:** Steady state GG levels in salt-acclimated cells of the WT, IsaR1OE and $\Delta isaR1$ strains. The data are presented as the means \pm SD of two biological replicates and integrate the measurements at 24 hours, 48 hours and 7 days after the salt shock for each strain. **C:** Suc accumulation kinetics of the same culture used for measuring GG kinetics (panel **A**). **D:** Relative levels of G3P in salt-acclimated cells of the respective strains measured by GC-EI-TOF-MS. Data represent the means \pm SD of *n* biological replicates as indicated. WT, *Synechocystis* wild type carrying an empty pVZ322-*PpetE::oop* plasmid backbone; IsaR1OE, strain carrying pVZ322-*PpetE::isaR1::oop* plasmid (overexpression strain).

Figure 5. Steady state levels of the *ggs* mRNA (A) and Ggs protein (B) in long-term iron-limited cells of the WT and mutant strains with absent ($\Delta isaR1$) or increased IsaR1 levels (IsaR1OE). To induce iron depletion, a 10-fold excess of the Fe-specific chelator DFB was added to the cells, which were then grown for a further 7 days. The medium was supplemented with 4% (w/v) NaCl and 2 μ M CuSO₄ throughout the experiment to ensure adequate *ggs* expression and ectopic expression of IsaR1 in the overexpression strain. L.c. – loading control, either excerpts of the corresponding ethidium bromide stained RNA gels showing the 16S rRNA (Northern blots) or an excerpt of a Ponceau-stained membrane showing the same size range of proteins (immunoblots). For each strain, two replicates are shown (1 and 2). **C:** Densitometric evaluation of the signals from panels **A** and **B** after normalization to the respective loading control. WT, *Synechocystis* wild type carrying an empty pVZ322-*PpetE::oop* plasmid backbone; IsaR1OE, strain carrying pVZ322-*PpetE::isaR1::oop* plasmid (overexpression strain); $\Delta isaR1$, *isaR1* deletion mutant.

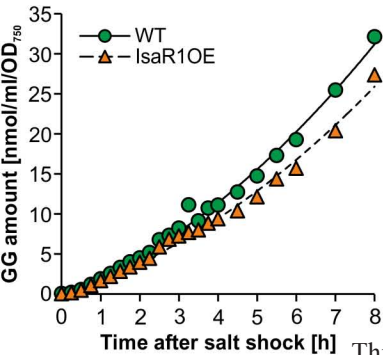
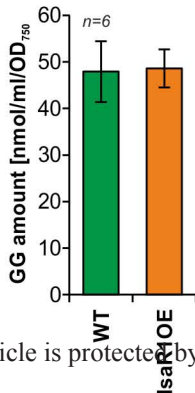
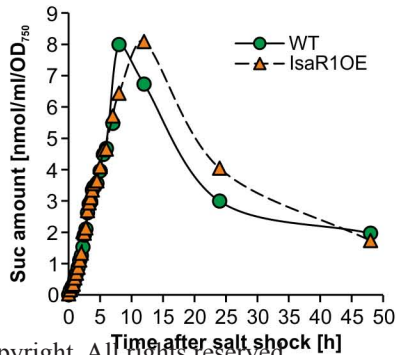
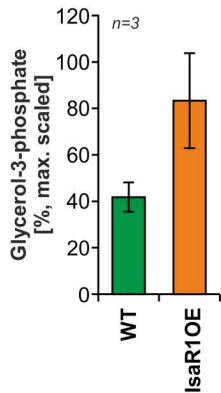
Figure 6. Expression kinetics of IsaR1 and *ggs* mRNA (A) or Ggs protein (B) in response to iron limitation. To induce iron depletion a 10-fold excess of the Fe-specific chelator DFB was added to the cells. To ensure adequate *ggs* expression the medium was supplemented with 4% (w/v) NaCl throughout the experiment. L.c. – loading control, either excerpts of the corresponding ethidium-bromide-stained RNA gels showing the 16S rRNA (Northern blots) or an excerpt of a Ponceau-stained membrane showing the same size range of proteins (immunoblots). **C:** Densitometric evaluation of the signals after normalization to the loading control. The respective values are indicated as the relative levels referring to the WT at time point 0 (prior to iron depletion, set to level of 1). WT, *Synechocystis* wild type carrying an empty pVZ322-*PpetE::oop* plasmid backbone; $\Delta isaR1$, *isaR1* deletion mutant.



A**B****C****D**

A**WT****IsaR1OE****B****C**

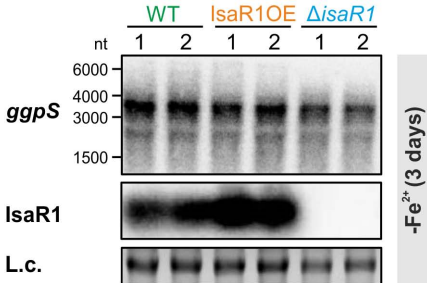
This article is protected by copyright. All rights reserved.

A**B****C****D**

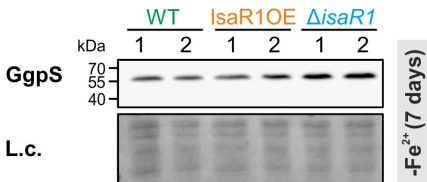
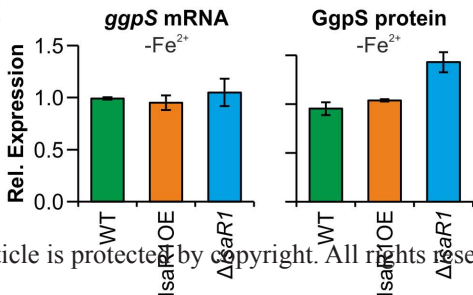
This article is protected by copyright. All rights reserved.

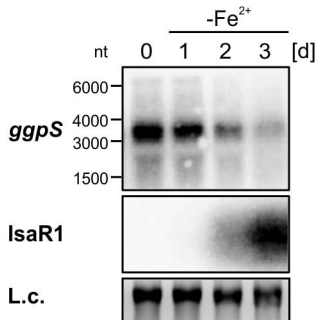
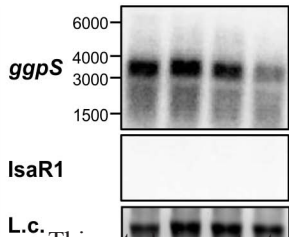
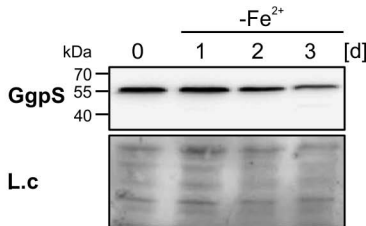
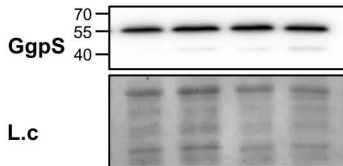
A

RNA level

**B**

Protein level

**C**

A**RNA level****WT** **Δ isaR1****B****Protein level****WT** **Δ isaR1****C**